Rev. Roum. Sci. Techn.– Électrotechn. et Énerg.
Vol. 63, 3, pp. 289–294, Bucarest, 2018

DUAL RANDOMIZED PULSE WIDTH MODULATION TECHNIQUE FOR BUCK CONVERTER FED BY PHOTOVOLTAIC SOURCE

AIMAD BOUDOUDA[1], NASSERDINE BOUDJERDA[2], ABDERRAZAKE AIBECHE[1], AHCENE BOUZIDA[1]

Key words: Randomized pulse width modulation, Photovoltaic system, Electromagnetic compatibility (EMC), Buck converter.

Randomized pulse width modulation (RPWM) is a technique used to spread the power spectrum over a wide frequency range; it aims to reduce the amplitudes of the power harmonics and consequently the conducted electromagnetic interferences (EMI). In this paper, a dual RPWM (DRPWM) scheme for the buck converter fed by a photovoltaic (PV) source, operating in discontinuous conduction mode (DCM) is proposed. It combines two simple schemes, random pulse position (RPPM) and random switching frequency modulation (RSFM). First, the modulating principle is presented and then, a general mathematical model of power spectral density (PSD) of the input current is derived and validated for the three schemes. The PSD analysis of the input current is carried out in order to show the advantage of the proposed scheme compared to the simple RPWM schemes. An application on a buck converter fed by photovoltaic source confirms that the proposed technique does not affect the solar PV buck converter performances, in the other side the randomization effect is confirmed and analyzed in steady-state characteristics of the buck converter, which is advantageous in reducing (EMI) in both input (PV source) and output (load).

1. INTRODUCTION

Dc/dc converters are widely used in several industrial applications. In recent years, they have become a key device in renewable energy applications such as photovoltaic (PV) systems. The buck converter is common in some renewable energy applications such as solar-powered dc motors and lighting systems [1]. Classically, the buck converter is controlled by deterministic pulse width modulation (DPWM) technique [2]. The rapid variations of the current in the power switches generate conducted electromagnetic interferences (EMI), which are conducted through the cables to the photovoltaic (PV) cell system, and from there on, they are radiated when the cells act as an antenna and will affect the sensitive equipment nearby [1, 3].

To better meet the EMC standards for conducted EMI, one can use the RPWM technique, which is one of the most effective and low-cost solutions: it has the advantage of spreading the power spectrum over a wide frequency range while significantly reducing its amplitude without any additional hardware in the circuit [4, 5]. Random PWM techniques (RPWM) have been developed for many years; they can be classified into two categories, including randomized switching frequency modulation (RSFM) and randomized pulse position modulation (RPPM). These schemes have been reported for both dc-dc [2, 4–11] and dc-ac [11–14]. It has been shown that RSFM allows a better spreading of the spectrum than RPPM and then offers more EMC efficiency [4, 6, 11, 12, 14]. However, for a maximum spreading of the spectrum, the combination of the two schemes (RSFM-RPPM) has also been proposed [6, 11, 12, 14]. Most of the previous cited works focused on the effect of RPWM techniques on output voltage and current only. Recently, with the emerging decentralized renewable energy sources more interest is being given to these techniques seen the double effect in both the input (i.e. renewable energy source) and the output of the converter [1, 4, 15, 16].

We propose a dual RPWM technique (RSFM-RPPM) for the control of a photovoltaic dc-dc converter.

The purpose is to analyze the efficiency of the proposed technique, both in spreading the power spectrum of the input current and in reducing its amplitude, in order to reduce the conducted EMI in the PV source side. At first, we propose the modulating principle of this technique. Then a general analytical model of the Power Spectral Density (PSD) of the input current is developed in DCM. Note that the simple schemes (RSFM and RPPM) are directly deduced as particular cases, from the proposed general model. This proposed analytical model is validated by comparison to simulation results under Matlab/Simulink with the use of the Welch estimation of the PSD which gives satisfactory results [12, 14]. Then, the PSD analysis shows that the proposed RPWM scheme allows better spreading of the PSD shape with smaller amplitude peaks compared to the simple schemes, which is the desired EMC advantage. Finally, we propose an application of RPWM in buck converter fed by solar PV panel; the effect of the randomization is highlighted in the waveforms of the PV current, buck input current and the output voltage as well as in the spread spectrum of the PV current and the buck input current for the purpose of reducing the conducted EMI.

2. MODULATING PRINCIPLE

2.1. CONVERTER STRUCTURE

The buck converter under study is schematized in Fig.1; it requires one switching signal q. It can operate in both continuous and discontinuous conduction modes [8].

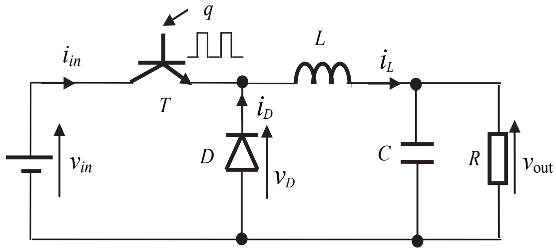

Fig. 1 – Buck converter.

The switching signal q is generally obtained by use of pulse width modulation (PWM) technique, in which a reference signal r is compared to a triangular carrier c (Fig. 2). For DPWM, the carrier c is fixed and for RPWM, the carrier is randomized.

[1] University of M'Hamed Bougara, Department of Electrical Systems Engineering, Algeria, E-mail: aimad.boudouda@gmail.com
[2] University of Mohamed Seddik Ben Yahia, Department of Electrical Engineering, Jijel, Algeria, E-mail: n_boudjerda@yahoo.fr

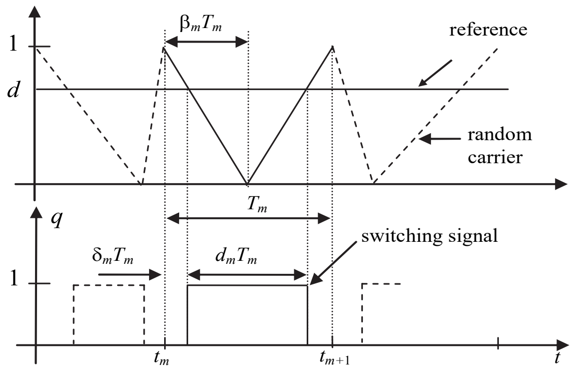

Fig. 2 – Modulating principle .

The switching signal q is completely characterized by three parameters (Fig. 2): the switching period T, (i.e. the period of the carrier), the duty cycle d and the delay report δ. In RPWM, these three parameters should be randomized in a combined or a separated way. In practice, d is generally deduced from a deterministic reference signal giving the control of the output voltage v_{out}. Thus, only the switching period T and the delay report δ can be really randomized.

From Fig. 2, for an arbitrary switching period of duration T_m, the delay report δ_m of the switching signal q can be expressed as follows:

$$\delta_m = \beta_m (1 - d). \qquad (1)$$

β_m is the fall time report of the carrier c in the m^{th} period.

A randomization of β_m in the interval [0, 1] gives random δ_m in the interval [0, (1 - d)] and the resulting position of the switching signal varies randomly from the beginning to the end of the period, (Fig. 2). Thus, the RPPM scheme is obtained by use of a triangular carrier with fixed period T and randomized fall time report β, (Fig. 2).

Random switching frequency modulation (RSFM) needs a triangular carrier with randomized period T between two values: $T_{\min}$ and $T_{\max}$. The randomization limits $T_{\min}$ and $T_{\max}$ of the period T are generally fixed around a mean value $\overline{T}$. For the buck converter, a saw tooth with a randomized period T is generally used ($\beta = 0$).

The proposed dual random modulation scheme (RSFM-RPPM) combines the two previous schemes; carrier parameters (T and β) are independently randomized in the intervals defined for the two simple schemes respectively (RSFM and RPPM). Related to the parameters T and β, the resulting RPWM schemes are summarized in Table 1.

Table 1
Resulting RPWM *schemes*

PWM schemes	β	*T*
DPWM	fixed [a]	fixed
RPPM	randomized	fixed
RSFM	fixed [a]	randomized
RSFM-RPPM	randomized	randomized

a: $\beta = 0$

2.2. CONTINUOUS AND DISCONTINUOUS CONDUCTION MODES

In the buck converter, the electronic switch (MOSFET or IGBT) chops both of the input current and the input voltage at high switching frequency; this is accompanied by an increase of high (dv/dt) and (di/dt). This causes high EMI and will affect the nearby electronic devices [2, 17]. The switching signal q is approximated with a square wave and the input current i_{in} may be approximated with a triangular wave in both of continuous and discontinuous conduction modes (Fig. 3), [2, 4].

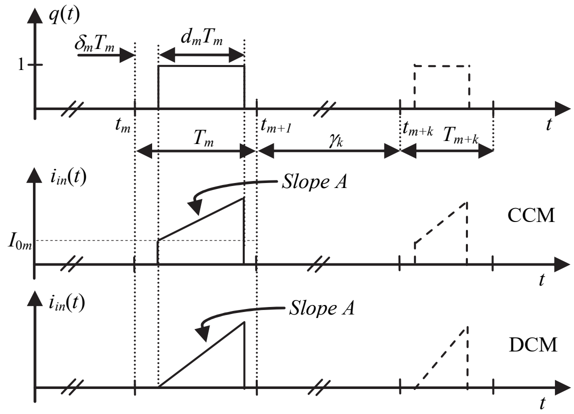

Fig. 3 – Switching signal and input current in CCM and DCM.

For a generic switching cycle m and under continuous conduction mode (CCM) and discontinuous conduction mode (DCM), the input current (i_{in}) can be expressed in a general form as follows: (note that $d_m = d$ = constant)

$$i_m(t - t_m) = \begin{cases} A \times (t - t_m - \delta_m T_m) + I_{0m}, & t_m + \delta_m T_m \le t \le t_m + \delta_m T_m + d T_m \\ 0, & \text{elsewhere} \end{cases} \qquad (2)$$

where:

t_m is the starting time of the m^{th} switching cycle

T_m is the m^{th} switching cycle

d is the m^{th} duty cycle

δ_m is the m^{th} delay report: $\delta_m = \beta_m \times (1 - d)$.

A is the slope of the rising edge: $A = \dfrac{v_{in} - v_{out}}{L}$, where:

$$v_{out} = \frac{1}{2}\left(\sqrt{\left(\frac{K}{v_{in}}\right)^2 + 4K} - \frac{K}{v_{in}} \right) \qquad (3)$$

and

$$K = \frac{(d v_{in})^2 RT}{2L}. \qquad (4)$$

I_{0m} is the initial value of the pulse at: $t = t_m + \delta_m T_m$. For DCM, $I_{0m} = 0$ and for CCM, $I_{0m} > 0$ (Fig. 3).

Note. It is important to note that the input current retains similar expressions for both CCM and DCM; the only difference is in the initial current (I_{0m}). This leads to similar spectral analysis. In practice, the CCM is generally obtained by increasing the inductor of the output filter (Fig. 1), which results in lower current ripple than DCM. In this paper we have restricted our study to DCM (high current ripple) in order to better show the effect of the RPWM in spreading the power spectrum.

3. SPECTRAL ANALYSIS OF INPUT CURRENT FOR DCM USING POWER SPECTRAL DENSITY

Generally, the analysis of random signals can be performed either by fast Fourier transform (FFT) or by PSD [14]. The FFT is originally discrete and leads to a continuous random spectrum, depending on the sample of the considered signal, thus the PSD is more appropriate for such signals and gives accurate results according to wiener-khintchine theorem; it can be expressed as follows [18]:

$$S(f)=\lim_{\tau\to\infty}\frac{1}{\tau}\mathrm{E}\left\{\left|\mathrm{F}[u_\tau(t)]\right|^2\right\}, \quad (5)$$

where:

$u_\tau(t)$ – considered signal during the time interval τ.

$\mathrm{F}[u_\tau(t)]$ – fourier transform of $u_\tau(t)$.

$\mathrm{E}\{.\}$ – statistical expectation.

3.1. ANALYTICAL EXPRESSION OF THE PSD (WIENER-KHINTCHINE THEOREM)

For a random pulse signal $i(t)$, belonging to the class of wide sense stationary (WSS) signals, expression (5) leads to the general expression (6), [4, 6, 11, 12, 14]:

$$S(f)=\lim_{N\to\infty}\frac{1}{\overline{T}}\mathrm{E}\left[\sum_{k=-N}^{N}I_m(f)I^*_{m+k}(f)\right], \quad (6)$$

where:

$\overline{T}$ _ statistical mean of the switching period;

$I_m(f)$ and $I^*_{m+k}(f)$ – the Fourier transform of the signal;

$i_m(t)$ – during the switching period T_m and its conjugate during the switching period T_{m+k}, respectively;

The expression (6) is developed as follows [4, 12]:

$$S(f)=\frac{1}{\overline{T}}\left\{\mathrm{E}\left[\left|I_m(f)\right|^2\right]+2\,\mathrm{Real}\left(\sum_{k=1}^{\infty}\mathrm{E}\left[I_m(f)I^*_{m+k}(f)\right]\right)\right\} \quad (7)$$

where $\mathrm{Real}(.)$ is the real-part of the expression in brackets.

During the switching period T_m, Fourier transform $I_m(f)$ of the current $i_m(t)$ given by expression (2) is:

$$I_m(f)=\frac{A}{(2\pi f)^2}\left\{\left[1+\mathrm{j}2\pi f d_m T_m\right]\mathrm{e}^{-\mathrm{j}2\pi f d_m T_m}-1\right\}\mathrm{e}^{-\mathrm{j}2\pi f\delta_m T_m}\,\mathrm{e}^{-\mathrm{j}2\pi f t_m}, \quad (8)$$

where $\delta_m=\beta_m\times(1-d_m)$.

Similarly, the complex conjugate $I^*_{m+k}(f)$ of $I_{m+k}(f)$ is:

$$I^*_{m+k}(f)=\frac{A}{(2\pi f)^2}\left\{\left[1-\mathrm{j}2\pi f d_m T_{m+k}\right]\mathrm{e}^{\mathrm{j}2\pi f d_m T_{m+k}}-1\right\}e^{\mathrm{j}2\pi f\delta_{m+k}T_{m+k}}\,\mathrm{e}^{\mathrm{j}2\pi f t_{m+k}}, \quad (9)$$

where $\delta_{m+k}=\beta_{m+k}\times(1-d_m)$.

After some mathematical transformations a closed form of the PSD can be obtained as follows [4, 6, 11]:

$$S(f)=\frac{1}{\overline{T}}\left\{\begin{array}{l}\mathrm{E}_T\left[\left|I(f)\right|^2\right]+\\ 2\mathrm{Real}\left(\dfrac{\mathrm{E}_{T,\beta}\left[I(f)\mathrm{e}^{\mathrm{j}2\pi fT}\right]\mathrm{E}_{T,\beta}\left[I^*(f)\right]}{1-\mathrm{E}_T\left[\mathrm{e}^{\mathrm{j}2\pi fT}\right]}\right)\end{array}\right\}, \quad (10)$$

where

$$I(f)=\frac{A}{(2\pi f)^2}\left\{\left[1+\mathrm{j}2\pi f dT\right]\mathrm{e}^{-\mathrm{j}2\pi f dT}-1\right\}\mathrm{e}^{-\mathrm{j}2\pi f\beta\times(1-d)T}. \quad (11)$$

3.1.1. PARTICULAR CASE OF RSFM SCHEME

The delay report ($\delta = 0$), thus a carrier with fixed fall-time report ($\beta = 0$) and randomized period T is used, which gives:

$$S(f)=\frac{1}{\overline{T}}\left\{\begin{array}{l}\mathrm{E}_T\left[\left|I(f)\right|^2\right]+\\ 2\mathrm{Real}\left(\dfrac{\mathrm{E}_T\left[I(f)\mathrm{e}^{\mathrm{j}2\pi fT}\right]\mathrm{E}_T\left[I^*(f)\right]}{1-\mathrm{E}_T\left[\mathrm{e}^{\mathrm{j}2\pi fT}\right]}\right)\end{array}\right\}. \quad (12)$$

3.1.2. PARTICULAR CASE OF RPPM SCHEME

The carrier has a fixed period T and a randomized fall-time report β, the resulting PSD expression is:

$$S(f)=\frac{1}{T}\left\{\begin{array}{l}\mathrm{E}_\beta\left[\left|I(f)\right|^2\right]+\\ 2\mathrm{Real}\left(\dfrac{\mathrm{E}_\beta\left[I(f)\right]\mathrm{E}_\beta\left[I^*(f)\right]\mathrm{e}^{\mathrm{j}2\pi fT}}{1-\mathrm{e}^{\mathrm{j}2\pi fT}}\right)\end{array}\right\}. \quad (13)$$

Note. For this scheme, at the multiples of the switching frequency $\left(f_k=\frac{k}{T},\ k=0,1,...\right)$, the denominator of expression (13) becomes $\left(1-\mathrm{e}^{\mathrm{j}2\pi k}=0\right)$, and the PSD (in Ampere²/Hertz), has discrete components with infinite amplitudes. Thus, it is suitable to decompose the expression (13) of PSD into two terms: a continuous term (continuous PSD) and a discrete one (power harmonics), [4]:

$$S(f)=\frac{1}{T}\left\{\begin{array}{l}\mathrm{E}_\beta\left[\left|I(f)\right|^2\right]-\left|\mathrm{E}_\beta\left[I(f)\right]\right|^2+\\ \dfrac{1}{T}\left|\mathrm{E}_\beta\left[I(f)\right]\right|^2\displaystyle\sum_{k=-\infty}^{+\infty}\delta\left(f-\frac{k}{T}\right)\end{array}\right\}, \quad (14)$$

where $\delta(\ )$ is the Dirac pulse.

3.1.3. PARTICULAR CASE OF DPWM SCHEME

In case of DPWM, the PSD contains only the discrete part (power harmonics in "Ampere²"):

$$S(f)=\frac{1}{T^2}\left|I(f)\right|^2\left(\sum_{k=-\infty}^{+\infty}\delta\left(f-\frac{k}{T}\right)\right). \quad (15)$$

3.2. WELCH APPROXIMATION OF THE PSD

In order to validate the analytical expressions of the PSD, the analysis of the input current is also carried out using a numerical method based on the estimation of Welch [19], applied on a representative sample of the input current after simulation of the buck converter. Note that the algorithm of Welch is available as the MATLAB utility "pwelch". This method is very satisfactory; it gives very good results compared to the measurement and to analytical ones [12, 14]. We will use this algorithm for validation by comparing between estimated PSD and computed PSD.

3.3. RANDOMNESS LEVELS

T and β are the random parameters using the probability density function $p(T)$ and $p(\beta)$ respectively, the expected operator $E[I(f)]$ should be expressed as follows:

$$E[I(T,\beta,f)] = \iint_{T\beta} p(T,\beta) I(T,\beta,f) \mathrm{d}T \mathrm{d}\beta, \tag{16}$$

where $p(T,\beta)$ is the probability density function of T and β. Random parameters T and β may take any probability law. In all our applications only uniform law is used because it's the simplest to implement. The lower and upper limits of random parameters T and β are defined by randomness level as follows:

– For RSFM: $R_T = \frac{T_{\max} - T_{\min}}{\overline{T}}$, T varies between $T_{\min}$ and $T_{\max}$, that gives:

$$T_{\min} = \overline{T}\left(1 - \frac{R_T}{2}\right) \text{ and } T_{\max} = \overline{T}\left(1 + \frac{R_T}{2}\right),$$

where $\overline{T}$ is statistic mean of switching period T. Theoretically, the maximum randomness level is obtained using $T_{\min} = 0$ and $T_{\max} = 2\overline{T}$, that means: $R_T = 2$. In practice R_T is fixed by practical considerations.

– For RPPM: $R_\beta = \frac{\beta_{\max} - \beta_{\min}}{\overline{\beta}}$,

where:

$\overline{\beta}$ – statistic mean of delay report β; β varies between $\beta_{\min}$ and $\beta_{\max}$.

Note. For the buck converter: $\beta_{\min} = 0$ and $\beta_{\max} = 1$ [6].

3.4. VALIDATION OF PSD MODELS

The validation of PSD models for the three RPWM schemes is performed by comparing the PSD computed analytically to that estimated by the Welch method based on the simulation of the converter in DCM with the following conditions [12, 14, 19]:

- Input voltage $v_{in} = 15$ V.
- Load ($R = 47\ \Omega$, $L = 165\ \mu$H, $C = 220\ \mu$F) for DCM.
- Duty cycle $d = 0.5$.
- The uniform probability law is used for to randomize the carrier parameters, as follows:

1. RSFM – the parameter β is fixed $(\beta = 0)$, and the period T is randomized in the interval $\left[\overline{T}\left(1 - \frac{R_T}{2}\right), \overline{T}\left(1 + \frac{R_T}{2}\right)\right]$, $\overline{T} = \left(\frac{1}{f_s}\right)$, $f_s = 20$ kHz and $R_T = 0.2$.
2. RPPM – T is fixed and β is randomized in the interval: $[0, R_\beta]$, with $\delta_{\min} = 0$ and $\delta_{\max} = 0.2$, gives $\beta_{\min} = 0$ and $\beta_{\max} = 0.4$.
3. RSFM-RPPM scheme – combination of two schemes RSFM and RPPM.

The results are given in Fig. 4.

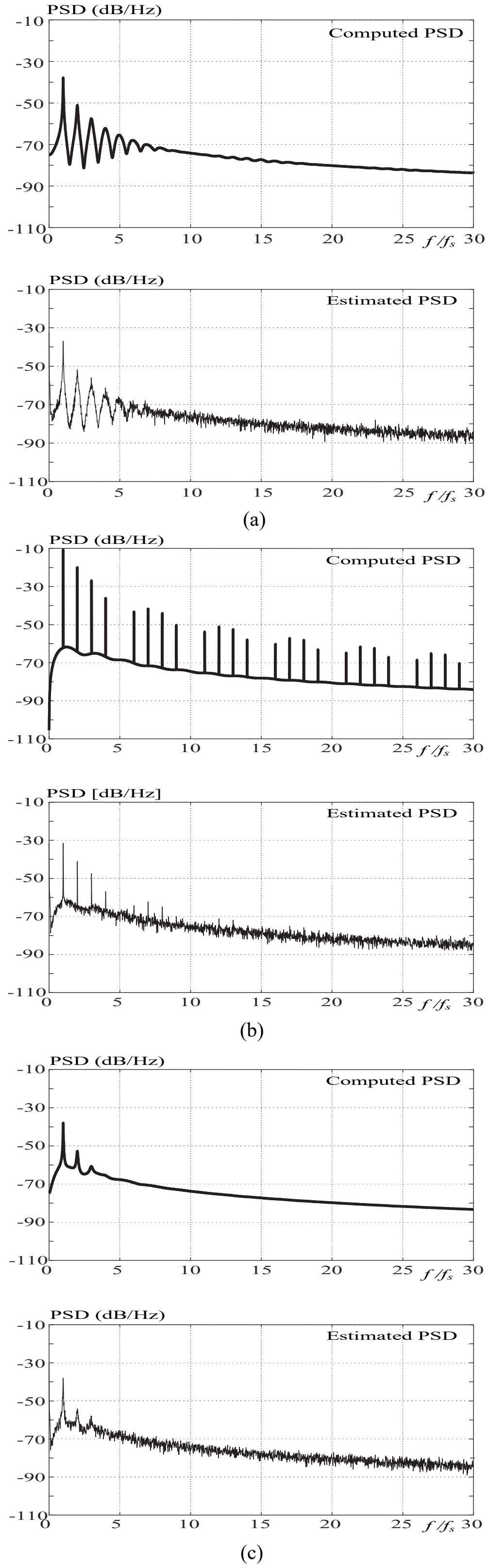

Fig. 4 – PSD of input current in DCM for (a) RSFM scheme, (b) RPPM scheme, (c) RSFM-RPPM scheme.

Figure 4 reveals perfect agreements between the computed PSDs by using the proposed models (expressions 10, 13 and 14) and the estimated PSDs (Welch method) for RSFM, RPPM and RSFM-RPPM respectively thereby validating our proposed model.

From Fig. 4b, RPPM scheme is not able to spread the PSD; it contains a continuous part (noise) and a discrete one (power harmonics), RSFM scheme gives a completely spread PSD that reduces considerably the amplitude of the peaks (Fig. 4a), thus RSFM scheme provides more EMC advantages than RPPM scheme and this is the intended purpose to better meet the EMC standards which limit the amplitudes of conducted EMI.

Fig. 4c shows clearly that the proposed scheme is more effective on spreading PSD and reducing its peaks; indeed the power spectrum is more spread with only a meaningful peak at the switching frequency f_s; this advantage is expected because the proposed scheme combines the properties of the two simple schemes (RSFM and RPPM).

4. APPLICATION TO SOLAR PV SYSTEM

To verify the effect of the proposed dual RPWM technique on the spreading of the power spectrum, an application in a buck converter fed by solar PV is proposed (Fig. 5). First, we compare the output voltage in both cases: deterministic and random PWM in order to see the influence of the modulation technique, second, we examine the EMC advantage of the random technique on both the output current of the PV solar (i_{pv}) and the input current (i_{in}) for the purpose of reducing the conducted EMI in both solar PV system and buck converter as shown in Fig. 5.

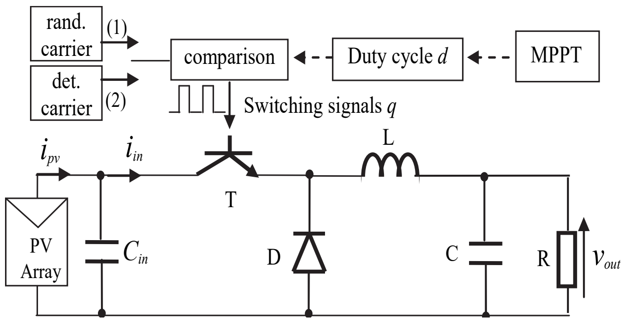

Fig. 5 – Schematic control of buck converter fed by PV solar.

Using SIMULINK software, a photovoltaic array of 30 modules in series is simulated. Each module has 36 cells in series. Table 2 summarizes the specifications of the used PV modules in standard conditions (1000 W/m^2 and 25°C) [20]. Figure 6 shows the current-voltage (*I-V*) and power-voltage (*P-V*) curves for standard conditions.

Table 2

Specifications of PV module MSX 60

Characteristics	Values
Rated power	60 W
Voltage at peak power	17.1 V
Current at peak power	3.5 A
Short-circuit current (I_{sc})	3.8 A
Open-circuit voltage(V_{oc})	21.1 V

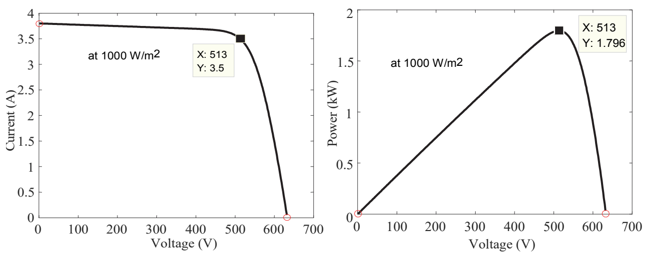

Fig. 6 – Characteristics of PV array at T = 25 °C.

4.1. EFFECT OF RPWM ON THE OUTPUT VOLTAGE OF THE BUCK FED BY THE PV SOURCE

Figure 7 shows the shapes of output voltage obtained by using the two techniques (deterministic PWM and RSFM-RPPM). Note that the PV source operates at the maximum power point (MPP).

In order to see the randomization effect, the two characteristics are given in the same figure (Fig. 7) for the two cases of modulation. It's clear that for a mean switching frequency (f_s = 20 kHz), there is practically no difference between the two techniques (Fig. 7a). The two voltages vary slightly around the mean value; the ripple doesn't exceed 1 V for a mean value of 467.5 V (Fig. 7b).

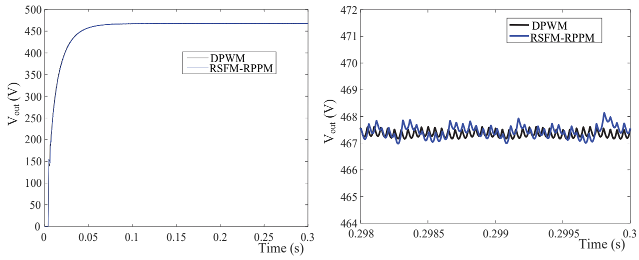

(a) Output voltage (b) Zoom on the steady state

Fig. 7 – Output voltage for DPWM and RSFM-RPPM.

4.2. EMC ADVANTAGE OF RPWM FOR SOLAR PV SYSTEM

In this section we are interested to the EMC advantage of RPWM. Indeed the purpose of this technique in solar PV system is to spread the spectrum of both buck input current and the PV output current, over a wide frequency range so as to mitigate the conducted EMI, knowing that this last is strongly correlated to the periodic waveforms of the current [4] and voltage [6, 11, 12, 14].

Figure 8 shows the buck input current in steady state and its PSD: the current is periodical and the PSD is principally formed by discrete power harmonics. In the other side random aspect appears clearly in the current of (Fig. 9a): there is no periodicity of the peaks. This appears clearly in the PSD (Fig. 9b) which is completely spread with an important reduction of the peaks which is required for reducing conducted EMI.

We also give in Fig. 10 the output current of the PV and its PSD: we clearly see the periodicity of the current for DPWM (Fig. 10a) which results in discrete power harmonics with important amplitudes (Fig. 10b). By using DRPWM, the PSD is spread with important reduction of peaks (Fig. 11b), which allows to reduce the size of the capacitive input filter C_{in} of the buck converter (Fig. 5).

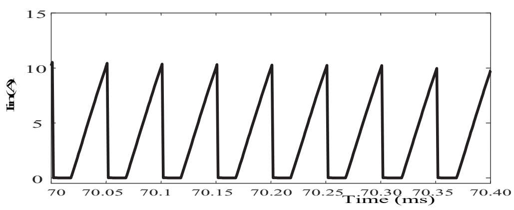

(a) Steady state current

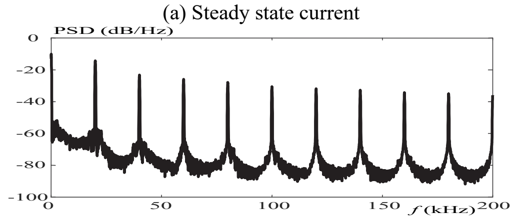

(b) PSD estimation (Welch method)

Fig. 8 – Input current waveform and PSD using DPWM

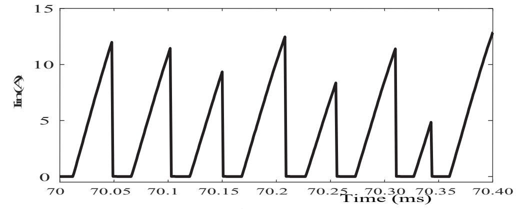

(a) Steady state current

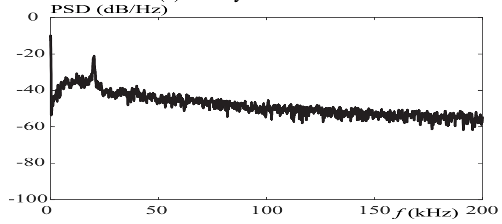

(b) PSD estimation (Welch method)

Fig. 9 – Input current waveform and PSD using DRPWM

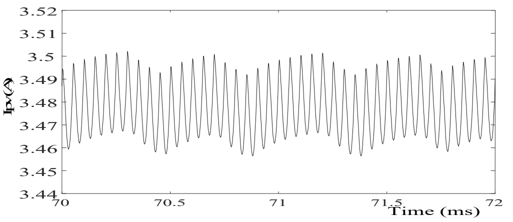

(a) Steady state current

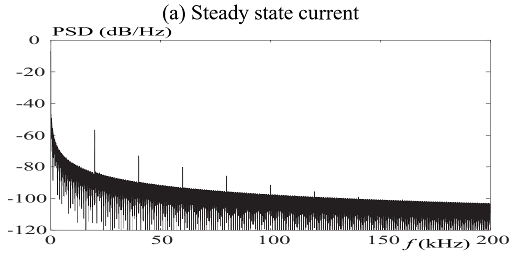

(b) PSD estimation (Welch method)

Fig. 10 – PV output current waveform and PSD using DPWM

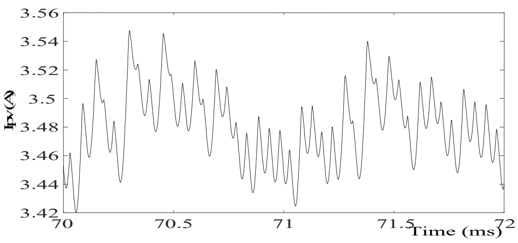

(a) Steady state current

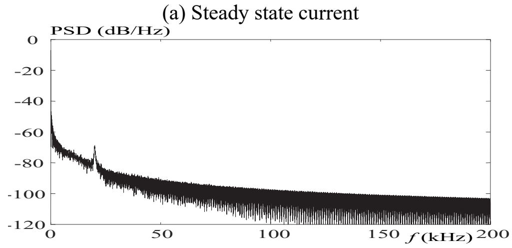

(b) PSD estimation (Welch method)

Fig. 11 – PV output current waveform and PSD using DRPWM

5. **CONCLUSIONS**

The conducted EMI generated by a buck converter using a DPWM technique has a discrete frequency spectrum with important amplitudes. In this paper, an alternative technique called dual randomized PWM is proposed in order to spread the spectrum of its input current. To make a rigorous analysis of the input current, we have developed and validated a general mathematical model of the power spectral density. The current analysis reveals that the proposed DRPWM technique realizes a better effective spreading of the PSD compared to the simple RPWM techniques and to the conventional DPWM technique, which is the sought EMC advantage. This technique is applied to a buck converter fed by solar PV system. The analysis of both the buck input current and the PV solar current confirms the beneficial effect of this technique.

Received on May 28, 2017

REFERENCES

1. K.K. Chittibabu, N.K. Alphones, *Analysis of conducted EMI with a standalone solar-powered DC motor*, Turkish Journal of Electrical Engineering & Computer Sciences, **21**, pp. 1260–1271 (2013).
2. E.N.Y. Ho, P.K.T. Mok, *Design of PWM ramp signal in voltage-mode CCM random switching frequency buck converter for conductive EMI reduction*, IEEE Transactions on Circuits and Systems-I, **60**, *2*, pp. 505–515 (2013).
3. M.C.Di. Piazza, C. Serporta, G. Tine, G. Vitale, *Electromagnetic compatibility characterization of the DC side in a low power photovoltaic plant*, IEEE ICIT '04, IEEE International Conference on Industrial Technology, Hammamet, Tunisia, Dec. 2004.
4. K.K. Tse, S.Y.R. Hui, H.C.So, *Spectral characteristics of randomly switched pwm dc/dc converters operating in discontinuous conduction mode*, IEEE Transactions on Industrial Electronics, **47**, *4*, pp. 759–769 (2000).
5. V. Kus, P. Drabek, T. Josefova, *Education strategy regarding the electromagnetic compatibility at low-frequency*, Rev. Roum. Sci. Techn. – Électrotechn. et Énerg., **61**, *1*, pp. 48–52 (2016).
6. N. Boudjerda, M. Melit, B. Nekhoul, K. El Khamlichi Drissi, K. Kerroum, *Reduction of conducted perturbations in DC-DC voltage converters by a dual randomized PWM scheme*, Journal of Communications Software and Systems, **5**, *1*, pp. 33–43 (2009).
7. V. Adrian, J.S. Chang, B.H. Gwee, *A randomized wrapped-around pulse position modulation scheme for DC-DC converters*, IEEE Transactions on Circuits and Systems, **57**, *9*, pp. 2320–2333 (2010).
8. F. Mihalic, *Improved EMC of switched-mode power converters with randomized modulation*, Automatika, **53**, *2*, pp. 173–183 (2012).
9. Y.S. Lai, B.Y. Chen, *New random PWM technique for a full-bridge DC/DC converter with harmonics intensity reduction and considering efficiency*, IEEE Transactions on Power Electronics, **28**, *11*, pp. 5013–5023 (2013).
10. C. Krishnakumar, P. Muhilan, M. Sathiskumar, M. Sakthivel, *A new random PWM technique for conducted-EMI mitigation on buck converter*, J Electr Eng Technol, **10**, 2015.
11. A. Boudouda, N. Boudjerda, K. El Khamlichi Drissi, K. Kerroum, *Spread spectrum in full bridge DC-DC/DC-AC converter by optimized dual RPWM scheme*, The Mediterranean Journal of Electronics and Communications, **10**, *1*, pp. 666–673 (2014).
12. N. Boudjerda, A. Boudouda, M. Melit, B. Nekhoul, K. El Khamlichi Drissi, K. Kerroum, *Spread spectrum in three-phase inverter by an optimised dual randomised PWM technique*, International Journal of Electronics, **101**, *3*, pp. 308–324 (2014).
13. A. Peyghambari, A. Dastfan, A. Ahmadyfard, *Selective voltage noise cancellation in three phase inverter using random SVPWM*, IEEE Transactions on Power Electronics, **31**,*6*, pp.1783–1794 (2015).
14. A. Boudouda, N. Boudjerda, K. El Khamlichi Drissi, K. Kerroum, *Combined random space vector modulation for a variable speed drive using induction motor*, Electrical Engineering, Archiv fur Elektrotechnik, **98**, *1*, pp. 1–15 (2016).
15. M.A. Al-Saffar, E.H. Ismail, *A high voltage ratio and low stress DC-DC converter with reduced input current ripple for fuel cell source*, Renewable Energy, pp. 1–9 (2014).
16. Sarah K. Ronnberg, Aurora Gil-de Castro, A.M. Munoz, M.H.J. Bollen, J. Garrido, *Solar PV inverter supraharmonics reduction with random PWM*, 11th IEEE International Conference on Compatibility, Power Electronics and Power Engineering, Cadiz, Spain, 2017.
17. M. Miloudi, A. Bendaoud, H. Miloudi, *Common and differential modes of conducted electromagnetic interference in switching power converters*, Rev. Roum. Sci. Techn. – Électrotechn. Et Énerg., **62**, *3*, pp. 246–251 (2017).
18. D. Middleton, *Introduction to statistical communication theory*, IEEE Press, 1996.
19. P. D. Welch, *The use of fast Fourier transform for the estimation of power spectra: A method based on time averaging over short, modified periodograms*, IEEE Trans on Audio and Electroacoustic, **Au-15**, pp. 70–73 (1967).
20. P. S. Sikder, N. Pal, *Incremental conductance based maximum power point tracking controller using different buck-boost converter for solar photovoltaic system*, Rev. Roum. Sci. Techn. – Électrotechn. et Énerg., **62**, *3*, pp. 269–275 (2017).